Available online at www.sciencedirect.com
SCIENCE DIRECT®
Journal of Catalysis 223 (2004) 444–453
JOURNAL OF CATALYSIS
www.elsevier.com/locate/jcat

Alkene chemistry on the palladium surface: nanoparticles vs single crystals

A.M. Doyle, Sh.K. Shaikhutdinov,* and H.-J. Freund

Department of Chemical Physics, Fritz-Haber-Institut der Max-Planck-Gesellschaft, Faradayweg 4-6, Berlin 14195, Germany

Received 1 December 2003; revised 16 February 2004; accepted 17 February 2004

Abstract

The adsorption of *trans*-2-pentene, *cis*-2-pentene, and 1-pentene on Pd(111) and Pd/Al_2O_3 model catalysts has been studied using temperature-programmed desorption (TPD). Each molecule reacts in an identical manner on the Pd(111) surface. Three distinct molecular adsorption states are observed, which have been assigned to multilayer, π-bonded pentene and interchanging di-σ-bonded pentene/pentyl groups. The latter species undergo coverage-dependent stepwise dehydrogenation. For *trans*-2-pentene on D_2 preadsorbed Pd(111), a H–D exchange reaction occurs, resulting in D-substituted pentene, which molecularly desorbs or dehydrogenates on heating similar to nonexchanged pentene. Pentane is not formed as a hydrogenation product on Pd(111). On Pd nanoparticles, dehydrogenation proceeds more readily than on Pd(111). In addition, the extent of the H–D exchange reaction is considerably greater on particles. In contrast to Pd(111), the hydrogenation reaction occurs on the Pd particles. Data show that di-σ-bonded pentene is the precursor for both the H–D exchange reaction and the pentane formation, with each occurring via a pentyl group. This pentyl group reacts either by β-H elimination to form pentene or by reductive elimination to form pentane. The results for pentenes are compared with those for ethene. We have found that, under the low-pressure conditions studied, alkene hydrogenation only occurs in the presence of subsurface hydrogen. The accessibility of the subsurface hydrogen atoms is enhanced on the particles, due to the nanoscale dimensions, relative to that on crystals. The results are rationalized on the basis of a model of overlapping desorption states, which may predict both the feasibility of alkene hydrogenation on Pd catalysts and the active species involved in the reaction.

Keywords: Hydrogenation; Alkene; Palladium; Temperature-programmed desorption; Subsurface hydrogen

1. Introduction

The selective hydrogenation of specific olefin bonds is required for numerous chemical processes, including petrochemical hydrotreating, fine chemical and pharmaceutical synthesis, and the treatment of fats in the food industry [1]. The general reaction mechanism proposed by Horiuti and Polanyi [2] in 1934 proceeds by (a) hydrogen dissociation on the metal surface, (b) alkene adsorption, (c) subsequent hydrogen addition to alkene, and (d) desorption of the product (alkane). More recently, the interactions of alkenes with metal surfaces have been studied on model catalyst systems with varying degrees of complexity, ranging from single crystals to metal particles deposited on oxide films [3–5].

Among unsaturated hydrocarbons, ethene seems to be the most intensively studied. The reactions of ethene with metal surfaces have been investigated on both single crystals and supported catalysts (see reviews of Zaera [6], and Sheppard and De La Cruz [7,8]). As Pd catalysts typically show high activities and selectivities, a considerable research effort has been devoted to studying surface reactions on Pd, employing infrared reflection absorption spectroscopy (IRAS), temperature-programmed desorption (TPD), high-resolution electron (and photoelectron) spectroscopy (HREELS, PES), and ab initio calculations [9–19].

Adsorbed ethene can form several dehydrogenated species, depending on metal surface symmetry, temperature, and coverage. The formation of ethylidyne ($\equiv C–CH_3$), ethynyl ($–C\equiv CH$), and vinyl ($–CH=CH_2$) species, as stable intermediates of ethene thermal transformations, has been

* Corresponding author.
E-mail address: shaikhutdinov@fhi-berlin.mpg.de (Sh.K. Shaikhutdinov).

0021-9517/$ – see front matter
doi:10.1016/j.jcat.2004.02.020

suggested on the Pd(111), Pd(110), and Pd(100) surfaces, respectively [15,18,19]. On highly dispersed Pd catalysts, ethene preferentially adsorbs in a π-bonded geometry at 90 K. However, it is the di-σ- rather than the π-complex that transforms into ethylidyne upon warming to room temperature [7,8]. Ethylidyne is present only as a spectator species during the hydrogenation reaction [20].

There is considerably less data on the interaction of higher hydrocarbons with Pd surfaces. Thornburg et al. [21] studied propene adsorption on clean Pd(111) by TPD and laser-induced thermal desorption. Propene mostly desorbs intact on heating: less than 10% of the adsorbed propene may dehydrogenate as evidenced by the hydrogen evolved during a TPD run. Recently, Stacchiola et al. [22] have found, using IRAS, that propene adsorbs in a di-σ configuration. On heating, propene dehydrogenates and forms coexisting propylidene and η^1-allyl species, the latter being favored. The authors reported that propane is formed during propene adsorption on a H_2 (D_2)-saturated Pd(111).

Madix and co-workers studied the reactions of ethene, propene, 1-butene, 1-hexene, and various dienes on the H(D) preadsorbed Pd(100) and Pd(111) surfaces by TPD [23,24]. They demonstrated that 1-alkenes undergo efficient H–D exchange for all C–H bonds below 300 K, whereas no hydrogenation products (alkanes) are observed. The exchange reaction was proposed to occur via the reversible hydrogenation of the adsorbed alkene to a half-hydrogenated intermediate. The absence of alkene hydrogenation was attributed to the stronger metal–hydrogen bond on Pd than other catalytically active metals (Pt and Rh), preventing further hydrogenation of the half-hydrogenated intermediate [24].

Metal particles deposited on thin oxide films represent more complex and realistic model catalyst systems than single crystal surfaces [4,25,26]. We have studied ethene adsorption on Pd particles vapor-deposited on a thin alumina film grown on NiAl(110) [27,28]. On D_2 preadsorbed particles, TPD results clearly showed ethane production at $\sim$ 200 K by the reaction, presumably, of π-bonded ethene with weakly bound hydrogen. We have also observed that the presence of subsurface hydrogen is the key species required for the hydrogenation reaction to occur. Recently, we have extended these studies to other alkenes on Pd/Al_2O_3 and compared the results with those for the Pd(111) crystal [29]. We have found that the hydrogenation reaction proceeds on the supported particles, while the Pd(111) crystal is inactive. The reactivity of the particles has been attributed to the enhanced accessibility of a subsurface hydrogen reservoir during reaction.

In this paper, we report a detailed and comparative study of different alkene (ethene, *trans*-2-pentene, *cis*-2-pentene, and 1-pentene) interactions with Pd(111) single crystal and Pd particles. The results are rationalized on the basis of a model of overlapping desorption states, which may predict the feasibility of alkene hydrogenation on Pd catalysts and the nature of the active species involved in the reaction.

2. Experimental

The experiments were performed in an ultrahigh vacuum chamber equipped with low-energy electron diffraction, Auger electron spectroscopy (AES, Omicron), and a differentially pumped quadrupole mass spectrometer (Fisons) for TPD measurements. The base pressure was below 1×10^{-10} mbar. Pd(111) and NiAl(110) single crystals were spot-welded to two parallel Ta-wires for resistive heating. The temperature was measured by a chromel–alumel thermocouple spot-welded to the backside of the crystal. Cooling to about 80 K was achieved by filling a manipulator rod with liquid nitrogen.

Pd(111) was cleaned by repeated cycles of Ar^+ ion sputtering and annealing to 1200 K. Surface carbon was removed by oxidation at 1000 K. The cleanliness was checked by AES and also by the absence of CO and CO_2 signals in the TPD spectra after O_2 adsorption at 300 K.

The thin alumina film was grown on the clean NiAl(110) by two cycles of oxidation in 10^{-6} mbar of O_2 at 550 K for 20 min and subsequent annealing to 1130 K for 4–5 min. Palladium (99.99%, Goodfellow) was deposited onto the alumina film at $\sim$ 300 K using a commercial evaporator (Focus EFM 3). The sample was biased with a retarding voltage in order to prevent metal ions from being accelerated toward the sample and creating nucleation centres on the surface. A deposition rate of 1 Å min^{-1} was used, as calibrated with a quartz microbalance. The amount of Pd deposited is presented in the text as a nominal thickness (in Å).

We found that hydrogen may adsorb on Pd particles from the vacuum background during Pd deposition. In order to remove this hydrogen, the sample was flashed to $\sim$ 400 K immediately following Pd deposition.

All gas exposures, measured in Langmuir (1 L $= 10^{-6}$ Torr s), were performed with a directional gas doser in order to minimize contamination of the vacuum chamber. The doser was calibrated by comparing TPD spectra of CO on the clean Pd(111) surface with spectra obtained by backfilling the chamber. Deuterium (99.9%, isotopic content 99.5%), oxygen (99.999%), and ethene C_2H_4 (99.5%) were supplied by AGA Gas, *trans*-2-pentene (99%) and 1-pentene (96%) by Fluka, and *cis*-2-pentene (98%) by Aldrich. Deuterated ethene, C_2D_4, (isotopic content 99%) was supplied by Isotec Inc. The pentene isomers were purified by repeated freeze-thaw cycles before adsorption.

The mass spectrometer had a differentially pumped shield with an aperture of 6 mm. For the TPD measurements, the nozzle of the shield was placed about 0.5 mm in front of the sample surface to minimize the signal coming from the sample heating wires. A linear temperature ramp with a heating rate of 5 K s^{-1} was generated using a feedback control system (Schlichting Phys. Instrum.).

It is well known that hydrocarbons exhibit a complex cracking pattern in the mass spectrometer, which depends on the ionization potential applied (typically 70 V), such that the most intense signal often appears as a fragment of the

mass corresponding to the molecular weight of the molecule. The fragmentation patterns can be found in the literature [30] or measured by the mass spectrometer. Therefore, in order to increase sensitivity, we used the following masses to analyze the hydrocarbon molecules: *trans*(*cis*)-2-pentene and 1-pentene C_5H_{10} (55), D-substituted pentenes $C_5H_{10-x}D_x$ (56 and 57 for $x = 1$ and 2, respectively), deuterated pentane $C_5H_{10}D_2$ (45). We have checked that these mass fully describe desorption of the corresponding molecules by simultaneously measuring the fragments and full mass signals in additional experiments. For reactions of deuterated ethene, we used the full mass signals.

Note that the different pentene isomers cannot be discriminated based on their fragmentation patterns. Therefore, we cannot follow any isomerization reactions with TPD. The TPD spectra presented here are not corrected for ionization gauge sensitivities. In all TPD experiments, deuterium was adsorbed at 200 K and pentene was adsorbed at 100 K. Note also that the clean alumina film did not show any reactivity toward ethene or pentenes.

3. Results and discussion

3.1. Trans-2-pentene on Pd(111)

A series of TPD spectra for *trans*-2-pentene is shown in Fig. 1 as a function of exposure at 100 K. Three distinct molecular desorption states, centered at 130 K (α), 175 K (β), and 260 K (γ), develop in the spectra with increasing pentene coverage. The H_2 evolution, shown in Fig. 1b, clearly demonstrates that dehydrogenation occurs over a wide range of temperatures and depends on pentene coverage. Three dehydrogenation regimes are observed. For an exposure of 0.02 L, H_2 desorption signals are found at 380 and 520 K with a broad shoulder present at higher temperatures. These peaks shift to 400 and 540 K, respectively, and additional peaks at 610 and 690 K emerge for increasing *trans*-2-pentene exposures to 0.11 L. At further increasing exposures, the signal proportionally scales until reaching saturation at ~ 0.33 L, and thereafter pentene starts to desorb molecularly, as seen in Fig. 1a.

The H_2 signals below 300 K simply follow the molecular desorption of pentene and are attributed to the fragmentation of pentene in QMS. (These signals are removed from the remaining figures for clarity.) For comparison, we show the TPD spectra of H_2 adsorbed on Pd(111) as an inset in Fig. 1a. Hydrogen exhibits a single desorption peak, which shifts to a lower temperature at increasing exposure. The H_2 signal from the pentene TPD has a similar intensity, but the desorption temperature is ca. 50 K higher, and gradually shifts to a higher temperature at increasing pentene exposure. Therefore, all H_2 peaks observed at 380–700 K for pentene adsorption are assigned to the reaction-limited desorption of hydrogen from the stepwise dehydrogenation of chemisorbed species.

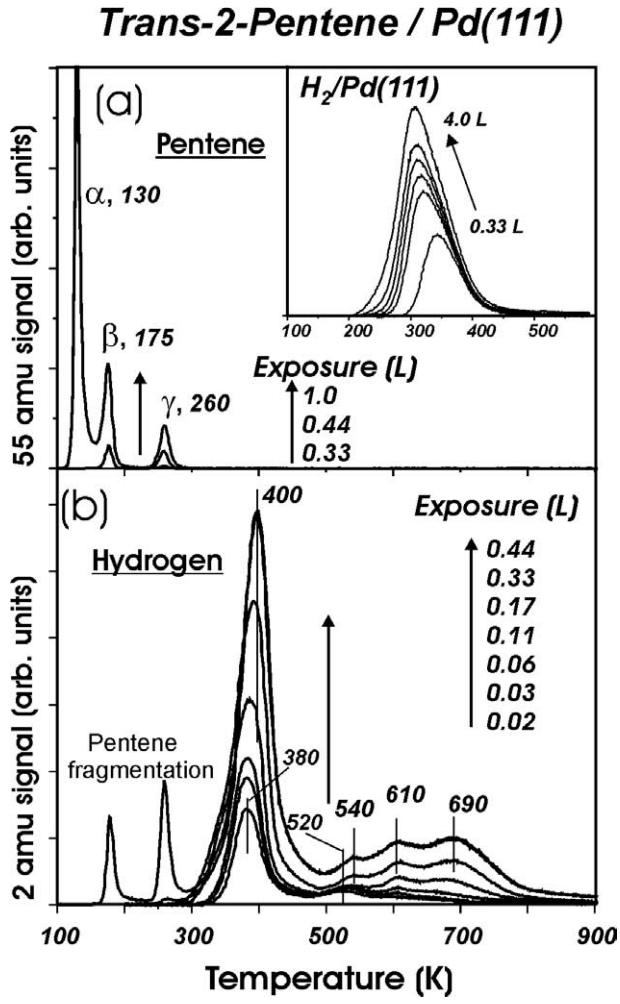

Fig. 1. TPD spectra of *trans*-2-pentene adsorbed on Pd(111) at 100 K as a function of exposure. The pentene (a) and hydrogen (b) desorption signals are shown. H_2 TPD spectra for clean Pd(111), adsorbed at 200 K, are shown as inset in (a).

The exposure dependence of the dehydrogenation temperatures may be explained by a different adsorption geometry of pentene as a result of specific interactions of neighboring molecules with increasing coverage. This effect has been demonstrated for various benzene derivatives (for example, see Ref. [31]).

3.2. Trans-2-pentene on D_2 preadsorbed Pd(111)

The Pd(111) surface was exposed to various quantities of D_2 and then to *trans*-2-pentene, and the resulting TPD spectra are shown in Fig. 2. Fig. 2a shows that the amount of pentene, desorbing from the γ state, decreases while the α and β signals gain intensity, as the D_2 coverage is increased. Fig. 2b shows that pentene-d_1 (C_5H_9D) desorbs at ~ 260 K, i.e., at the same temperature as the γ state of pentene (C_5H_{10}). This finding indicates that H–D exchange takes place, and the exchanged molecule has the same precursor as pentene desorbing from the γ state on the clean surface. A smaller quantity of pentene-d_2 also desorbs from

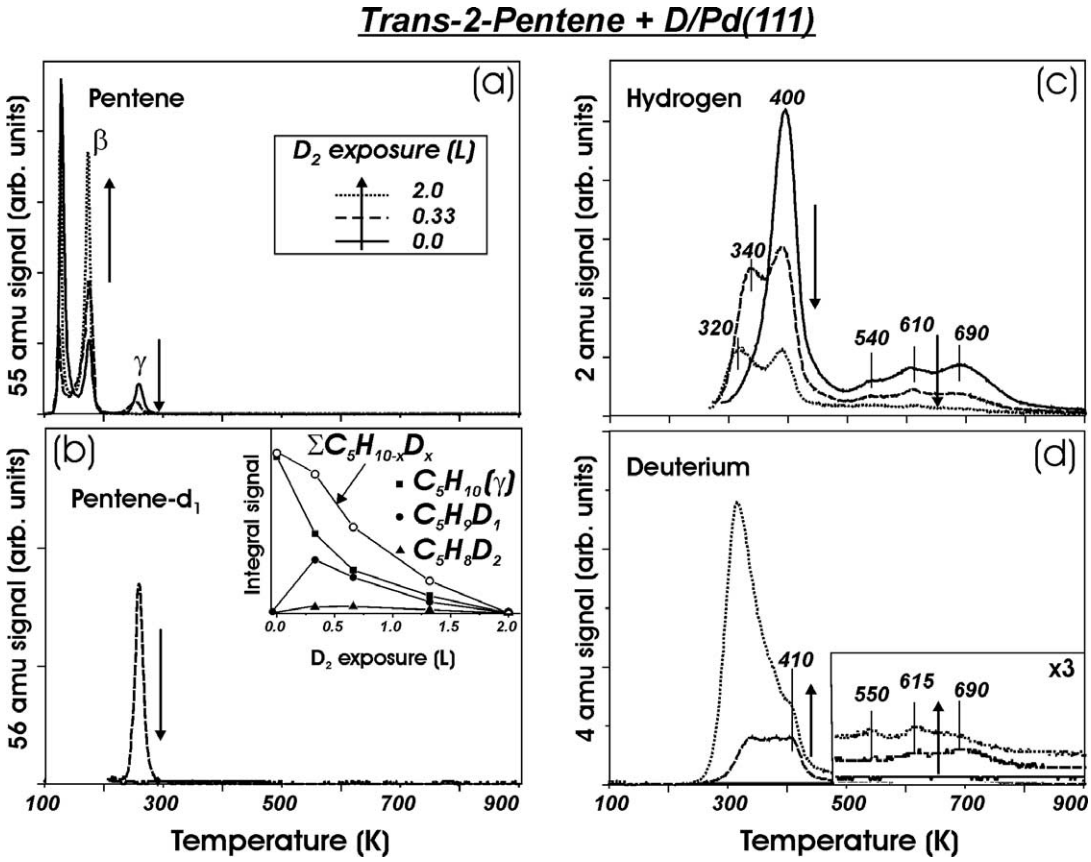

Fig. 2. TPD spectra of 1 L *trans*-2-pentene adsorbed on D_2 preexposed Pd(111) as a function of D_2 exposure: (a) pentene, (b) pentene-d_1, (c) H_2, and (d) D_2. The integral TPD areas for pentene, pentene-d_1, pentene-d_2, and total pentene desorbing from the γ state are shown as an inset in (b).

the γ state. Pentene containing 3 deuterium atoms or more was not reliably detected.

The amount of pentene-d_1 decreases with increasing D_2 preadsorbed in an analogous manner to that observed for pentene desorption. The integrated TPD signals for pentene, pentene-d_1, and pentene-d_2 are plotted as a function of D_2 exposure in the inset in Fig. 2b. Since neither pentene from the γ state nor D-substituted pentene are detected for 2 L D_2 exposure, we can conclude that saturated D_2 exposure actually suppresses pentene chemisorption in the γ-state on Pd(111). (Note that such a blocking effect may explain why Stacchiola et al. did not observe H–D exchange for propene adsorption on the 10 L D_2 preexposed Pd(111) surface [22].)

The H_2 desorption signal, shown in Fig. 2c, also demonstrates the H–D exchange reaction, as a new hydrogen peak at 320–340 K emerges, while desorption at $T > 400$ K is identical to that observed for pure *trans*-2-pentene adsorbed on clean Pd(111). This new peak is desorption-limited, and arises from the recombination of H ad-atoms released during the exchange reaction of H in pentene with D atoms preadsorbed on the Pd surface.

The D_2 signal, shown in Fig. 2d, is very similar to the H_2 signal. The D_2 signal at around 300 K is desorption limited, while the desorption features at 550, 615, and 690 K are certainly due to the dehydrogenation of D-exchanged pentene molecules. It seems likely that the peak at 410 K is also reaction limited, although it overlaps with the desorption of nonreacting preadsorbed D_2 molecules at 200–400 K (see inset in Fig. 1).

As the D_2 exposure increases, the total amount of desorbing hydrogen is decreased, in agreement with site blocking effect of D_2 on pentene chemisorption in the γ state. The quantities of D_2 formed during dehydrogenation above ~ 450 K increase only slightly. Therefore, the dehydrogenation route cannot account for the decrease of molecular desorption from the γ state (see inset in Fig. 2b).

Only negligible quantities of pentane were found under these conditions, thus indicating that hydrogenation does not practically occur on Pd(111). The hydrogenation was also not detected in the reverse experiment, i.e., when *trans*-2-pentene was adsorbed on Pd(111) and then exposed to D_2.

3.3. Cis-2-pentene and 1-pentene on Pd(111)

The adsorption of *cis*-2-pentene and 1-pentene on clean and D_2 preadsorbed Pd(111) is summarized in Fig. 3. In general, the adsorption characteristics and reactions are identical to those of *trans*-2-pentene. Again, three desorption states are found at 130, 170, and 255 K as shown in Figs. 3a and c. Dehydrogenation of both alkenes on clean Pd(111) results in H_2 evolution at 395, 540, 610, and 690 K as shown in Figs. 3b and d, i.e., identical to those recorded for *trans*-

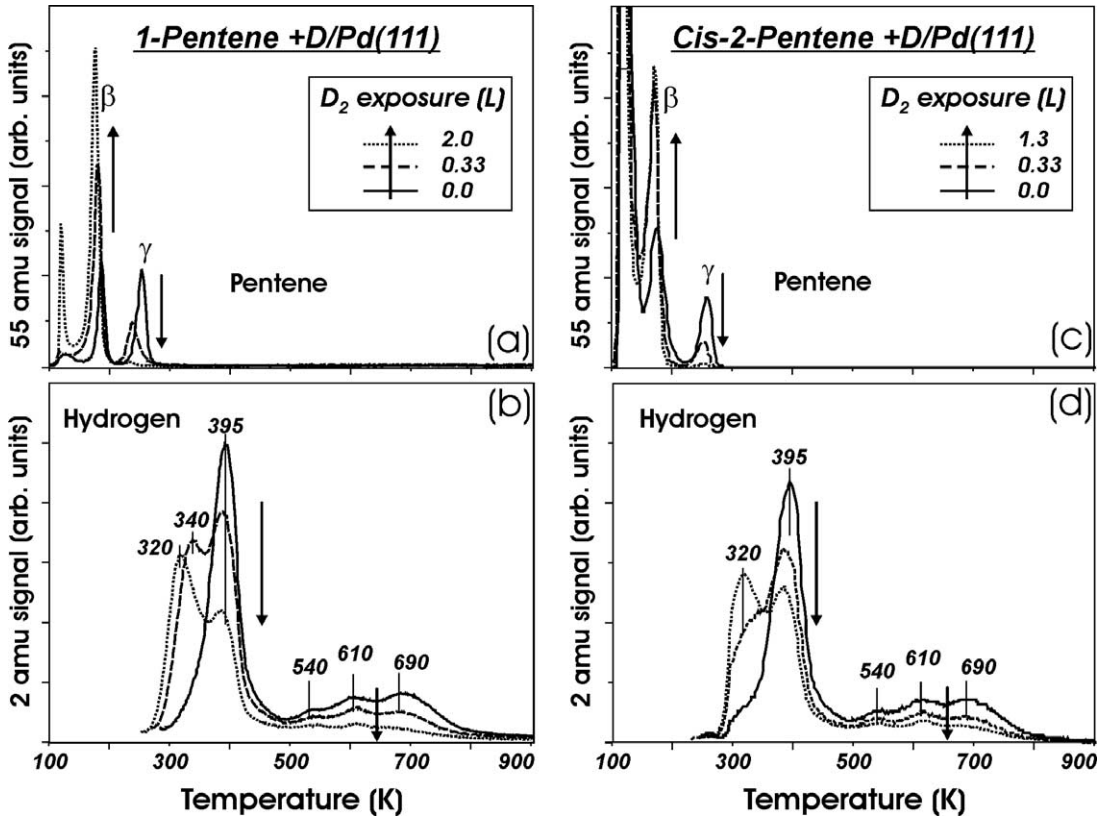

Fig. 3. TPD spectra of 1 L 1-pentene (a,b) and 0.66 L *cis*-2-pentene (c,d) adsorbed on D_2 preadsorbed Pd(111) at different D_2 exposures.

2-pentene. Therefore, we conclude that all three molecules dehydrogenate in an identical manner. H–D exchange is confirmed by the detection of desorption-limited H_2 at 320–340 K, which is characteristic for this reaction (cf. Fig. 2c and Figs. 3b and d).

3.4. Ethene on Pd(111)

Fig. 4a shows the TPD spectrum of ethene after exposure of 1.5 L C_2D_4 on clean Pd(111). A few distinct molecular desorption states are observed. A broad signal with a maximum at $\sim$ 280 K saturates at 0.1 L. With increasing ethene exposure, two sharp peaks centered at $\sim$ 200 and $\sim$ 170 K are detected, which, to our knowledge, have not been previously reported. In order to explain the origin of these features, we have performed a LEED study of the ethene/Pd(111) surface. A number of complex LEED patterns at ethene coverage above 0.2 L at 90 K are observed. In order to correlate the LEED and TPD data, we recorded a LEED movie on heating using the same heating rate as TPD. The results show that ethene forms different temperature-dependent ordered structures, which disappear at the same temperatures as the sharp peaks in the TPD spectrum shown in Fig. 4a. Therefore, these peaks are attributed to order-disorder phase transitions on heating and will be discussed in more detail in a forthcoming paper (A.M. Doyle, S.K. Shaikhutdinov, H.-J. Freund, in preparation).

Ethene dehydrogenation on Pd(111) is clearly seen in Fig. 4a by the presence of D_2 evolution. The D_2 desorption above 400 K provides direct evidence for the dehydrogenation process.

Fig. 4b shows that ethene undergoes extensive H–D exchange on D_2 preadsorbed Pd(111), since all possible deuterated molecules $C_2H_{4-x}D_x$ ($x = 0$–4) are detected. The desorption temperature shifts from 275 to 300 K for ethene-d_1 to ethene-d_4, respectively. These findings confirm that H–D exchange occurs by the addition and loss of H(D) atoms to di-σ-bonded ethene, i.e., a dynamic ethene/ethyl transformation occurs. We have also observed only trace quantities of ethane desorbing at 270 K.

3.5. Alkene adsorption on Pd(111) and D/Pd(111): general trends

The TPD data presented in Sections 3.1–3.4, for the adsorption of different alkenes on Pd(111), show that the results are essentially identical for the different pentene isomers, and that the pentene desorption occurs from three distinct states. At low temperatures and high exposures pentene may form a condensed (or multilayer) film from which it desorbs at $\sim$ 130 K (α state). Weakly bonded pentene, presumably in a π-configuration, desorbs at $\sim$ 170 K (β state). Accordingly, the high-temperature γ state is associated with di-σ-bonded molecules. D_2 preadsorption reduces the quantity of pentene desorbing from the γ state and favors molec-

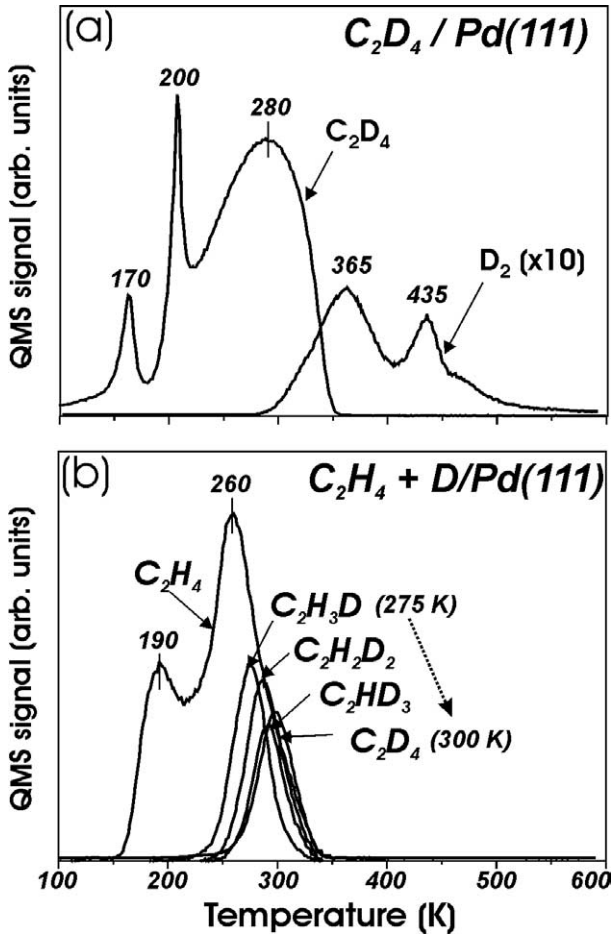

Fig. 4. (a) TPD spectra of 1.5 L ethene C_2D_4 adsorbed at 100 K on Pd(111): C_2D_4 and D_2 signals are shown. (b) TPD spectra of 0.1 L ethene adsorbed on 0.2 L D_2 preadsorbed Pd(111). Formation of all ethene-d_x ($x = 0$–4) is detected.

ular desorption from the β state. This finding is in agreement with the observations that hydrogen preadsorption favors π-bonding of alkenes [9,12,13]. In addition, the reduced desorption from the γ state is also caused by its reaction with preadsorbed D, thus resulting in D-substituted pentene molecules either desorbing or dehydrogenating at the same temperatures as nonexchanged pentene (see Fig. 2).

Madix and co-workers suggested that the highest desorption temperature ($\sim$ 250 K) of 1-hexene from Pd(111) originated from the β-H elimination of half-hydrogenated di-σ-bonded 1-hexene, i.e., a hexyl group [24]. For the pentene isomers analyzed here, the presence of a covalently bonded pentyl group, which forms by the reaction of di-σ-bonded pentene with H(D) ad-atoms, would explain the H–D exchange observed. The di-σ-bonded pentene may form pentyl groups if there are H(D) atoms available. On the H(D)-free surfaces, the di-σ-pentene seems to desorb directly. Therefore, in general, the γ state corresponds to pentene/pentyl species on the Pd surface.

It should be noted that Chrysostomou and Zaera [32], using IRAS, observed the formation of a π-allyl species for propene adsorbed on the D precovered Pt(111) surface. The π-propyl group is believed to hydrogenate on heating to form di-σ-bonded propene, and subsequently undergoes multiple propene-propyl-propene conversions to produce extensive H–D-exchanged products. Therefore, in our experiments from TPD alone, the presence of a π-pentyl group cannot be excluded.

Ethene reactivity on Pd(111) also fits well with the scheme that di-σ-bonded ethene is the precursor for the H–D exchange reaction as previously found on Pd(100) [23]. Sekitani et al. also presented experimental evidence that this reaction occurred on the Pd(110)–H(2×1) surface via ethyl species [33].

3.6. Trans-2-pentene on $Pd/Al_2O_3/NiAl(110)$

The morphology of the Pd particles has been previously studied in our laboratory by scanning tunnelling microscopy (STM) and reported in detail in Refs. [25,27]. The particles, formed by room temperature deposition and of ca. 5 nm in average diameter, are mostly nucleated at line defects (domain boundaries and steps) of the alumina substrate. The particles are well defined and expose mainly (111) facets as illustrated by the STM image in Fig. 5a. Therefore, we can compare the results for Pd(111) with the well-faceted particles to study size effects for alkene reactivity on Pd. Note, that the Pd/alumina stability toward heating is limited to $\sim$ 600 K. At higher temperatures, strong sintering and metal migration into the support occur [34]. Therefore, we have conducted TPD studies on the Pd particles to 600 K only.

Fig. 5 shows the TPD results of *trans*-2-pentene adsorption on clean Pd particles as well as on particles preexposed with various quantities of D_2. The pentene desorption signal is shown in Fig. 5a. As in the case of Pd(111), γ (at 230 K) and β (at 165 K) states are observed. At lower temperatures, the signal from Pd overlaps with that of the alumina film, and both are assigned to the formation of a condensed film.

A desorption-limited H_2 peak centered at 265 K is detected as shown in Fig. 5b. This means that dehydrogenation commences below 265 K on Pd particles, which is at least 130 K lower than on Pd(111) (see Fig. 1b). A stepwise dehydrogenation is evidenced by the reaction-limited desorption peaks of H_2 at 410 and 510 K.

In coadsorption experiments, the γ signal decreases with increasing D_2 exposure, while the β peak increases. The main H_2 signal at 265 K does not shift in the presence of D_2, and therefore it may originate from both *trans*-2-pentene dehydrogenation and the H–D exchange reaction. Dehydrogenation of D-exchanged molecules is clearly seen by D_2 desorption peaks at 420 and 505 K. The decrease of the H_2 signal and simultaneous increase of the D_2 signal at $T > 350$ K with increasing D_2 exposure are due to an increase in the extent of H–D exchange.

In principle, these results are similar to those obtained on Pd(111). Considering the conclusions from the experi-

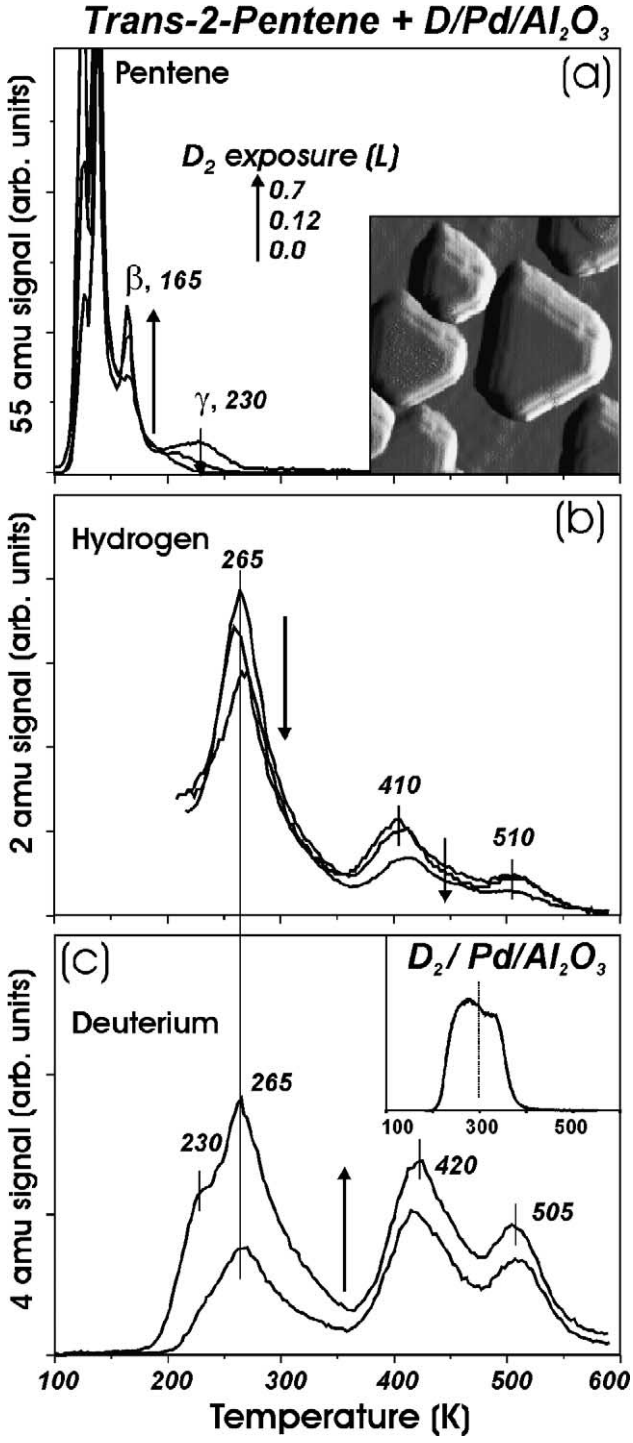

Fig. 5. TPD spectra of 0.7 L *trans*-2-pentene adsorbed at 100 K on D_2 preadsorbed Pd/Al_2O_3 as a function of D_2 exposure: (a) pentene, (b) H_2, (c) D_2. Palladium (4.9 Å of equivalent thickness) was deposited at 300 K. Particles are well faceted and mainly expose (111) surface as shown in 10×10 nm^2 STM image (inset in (a)). D_2 TPD spectrum after 0.7 L D_2 adsorption is shown as inset in (c).

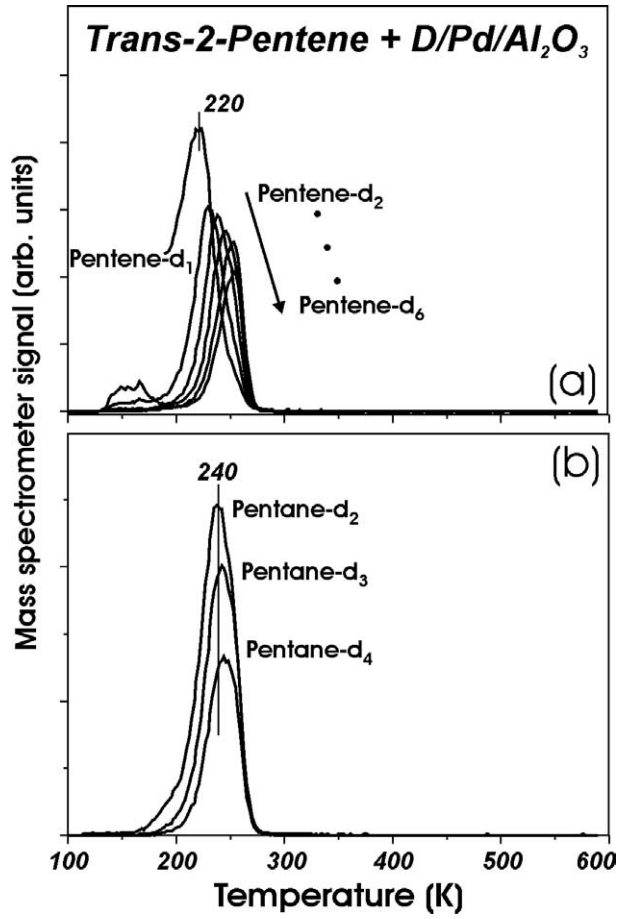

Fig. 6. Deuterated pentene (a) and pentane (b) isomers formed on Pd/Al_2O_3 for coadsorption of 0.7 L D_2 at 200 K and 0.5 L *trans*-2-pentene at 100 K. Pd (4.9 Å of nominal thickness) was deposited at 300 K. Extensive H–D exchange and pentane formation are observed.

ments on Pd(111), the pentene peak at 230 K is attributed to desorption from an interchanging pentyl/pentene group. Accordingly, desorption at 165 K is associated with π-bonded pentene, and the peaks below 150 K are due to the formation of multilayer pentene on both the Pd particles and the alumina film.

Fig. 6a shows that deuterated pentenes desorb on the particles from the γ state only, and pentene molecules containing up to six D atoms are detected. Therefore, the extent of H–D exchange on particles is significantly greater than on Pd(111), where pentene with only one and two D atoms was reliably detected. The exchange of 6 D atoms with pentene means that the reaction extends to at least 3 carbon atoms of the pentyl/pentene group. This finding may be interpreted such that the pentyl/pentene group "walks" on the surface by changing the carbon atoms anchored to the surface.

A more dramatic difference between Pd particles and Pd(111) is the formation of pentanes on D_2 preadsorbed Pd particles. Pentane-d_2 ($C_5H_{10}D_2$), pentane-d_3, and pentane-d_4 are all detected at around 240 K as shown in Fig. 6b. Note that we have previously reported that the Pd particles also hydrogenate ethene under the same conditions [27]. Therefore, the results clearly show that the Pd particles exhibit hydrogenation activity in contrast to a Pd(111) single crystal, which is inactive under the conditions studied.

Since alkene hydrogenation was not observed on other Pd single crystal surfaces as well, the presence of different facets cannot explain the exceptional activity of the particles. Of course, one must consider the low-coordinated atoms present on the particles such as corner and edge atoms. We have examined a roughened Pd(111) surface created either by ion sputtering or by vapor deposition of Pd in the same manner as we deposit Pd on alumina, following thermal flashing to 400 K. Based on the observation of the relatively diffuse LEED pattern, we conclude that the surface became less ordered than the well-annealed crystals. However, for the roughened surfaces, we have only observed negligible amounts of alkane, which are much lower than on Pd particles.

Comparing Fig. 1a and Fig. 5a, we see that the interaction of *trans*-2-pentene with Pd(111) and Pd particles does not differ significantly. Since the particle surface is less ordered than the single crystal, the desorption peaks on the particles are broader and less resolved. However, the desorption temperatures are very close to that observed on Pd(111). Therefore, the major difference in the reactivity of the two systems lies in their interaction with hydrogen rather than the alkene. The lack of alkene hydrogenation on Pd single crystals has been discussed in the literature [23] when compared to results on Pt, which is active for various alkenes. It was suggested that the strength of the metal–hydrogen bond could be responsible for such a difference, because a distinctly different mechanism seems unlikely.

It is well known that H_2 readily dissociates on Pd, and H atoms then migrate into the subsurface region and into the bulk occupying interstitial sites [27,35–42]. Based on the TPD studies, we have previously reported that the Pd particles contain a significant fraction of H(D) which is more weakly bound than on Pd(111) [27] (see also Fig. 8). In our opinion, the low temperature states below 300 K, observed for the particles, are associated with surface hydrogen, which is more weakly bound due to the presence of subsurface hydrogen. On heating, this weakly bound hydrogen on the surface desorbs first and is then repopulated from the subsurface hydrogen reservoir. On further heating, only surface hydrogen is present which desorbs at a higher temperature.

The Pd(111) crystal also contains surface and subsurface hydrogen at these exposures [36]. However, when H_2 is exposed to Pd crystals above 200 K, the H atoms can diffuse so deep into the bulk (up to 100 nm) that they cannot be released during a TPD run [37,38]. On particles of nanometer size, all hydrogen atoms are accumulated within the particles in close vicinity to the surface, as the particle size is much smaller than the diffusion length. As a result, both surface and subsurface hydrogen can be detected in the TPD spectra of the particles. (It should be noted that spillover of hydrogen onto the alumina support was not observed [43].)

In order to determine which hydrogen adsorption state is responsible for the superior activity of Pd particles we have performed coadsorption experiments with various amounts of D_2 preadsorbed. (Note that for each experiment a new sample was identically prepared. The reproducibility was proved by CO and D_2 TPD, and also by AES.)

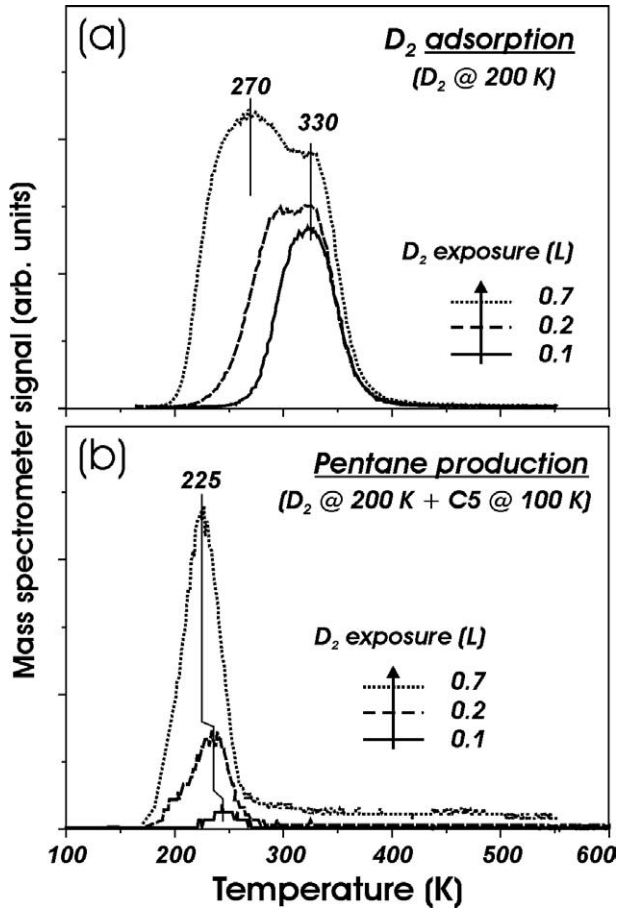

Fig. 7. (a) D_2 TPD spectra observed on identically prepared Pd/Al_2O_3 samples prior to coadsorption experiments. (b) Desorption signals of pentane-d_2 formed on the same samples preexposed to the same amount of D_2 as on (a) and subsequently exposed to 0.5 L *trans*-2-pentene at 100 K. Pentane is detected only in the presence of weakly bound D_2.

At low D_2 exposure, only the surface state is observed, thus resulting in a single desorption peak at $\sim$ 330 K as shown in Fig. 7a. At saturated exposures, the weakly bound D atoms are populated which give rise to D_2 desorption at 200–300 K. Fig. 7b shows the corresponding TPD spectra of pentane-d_2 produced on these samples in the coadsorption experiments with the same D_2 preexposure as used for the D_2 TPD spectra shown in Fig. 7a. Comparing these spectra, we see that pentane is only detected in the presence of subsurface D. In addition, the pentane desorption temperature is gradually shifted from 245 to 225 K, apparently following the onset of D_2 desorption in the D_2 TPD spectra. It is clearly seen that the amount of pentane formed is determined not by the total amount of D_2 preadsorbed but rather by the amount of weakly bound D_2. Previously, we have observed the same effects for ethene hydrogenation on Pd particles: the ethane production was about an order of magnitude lower in the deficiency of subsurface D [27]. Therefore, the TPD results provide strong evidence that the

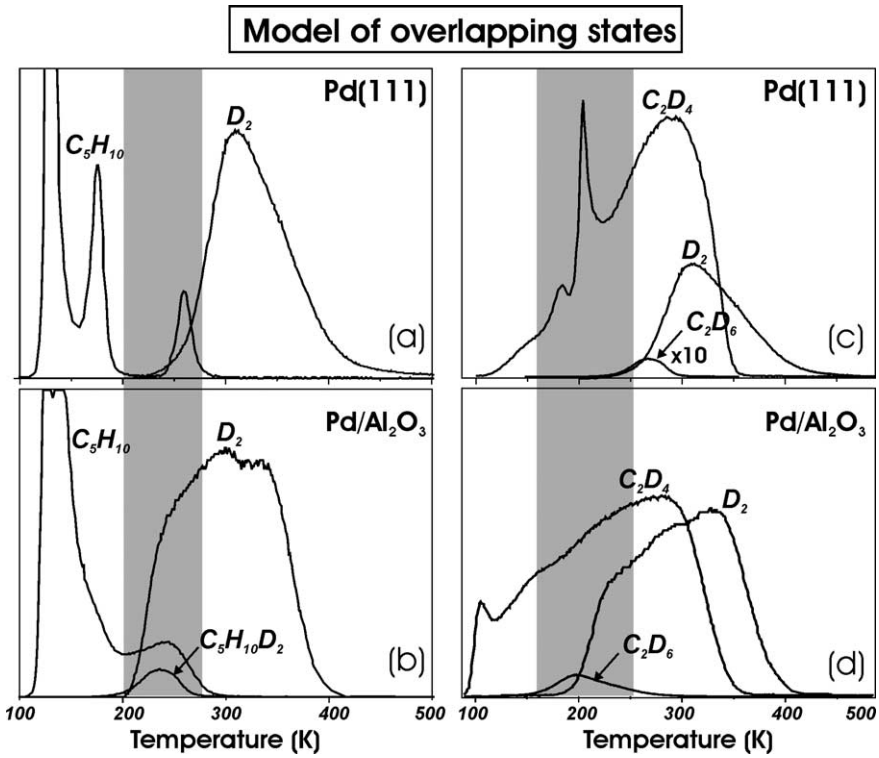

Fig. 8. (a) TPD spectra following individual adsorption of 1 L *trans*-2-pentene and 2 L D_2 on Pd(111) and production of pentane-d_2 during coadsorption of 0.5 L *trans*-2-pentene and 1 L D_2 on Pd(111). (b) Similar to (a) for 4.9 Å Pd on Al_2O_3. Exposures are 0.7 L of *trans*-2-pentene and 0.7 L of D_2. (c,d) TPD spectra following individual adsorption of 1 L ethene and 2 L D_2 and production of ethane-d_2 during coadsorption of 1 L ethene and 2 L D_2 on Pd(111) (c) and for 1.4 Å Pd on Al_2O_3 (d).

presence of weakly adsorbed hydrogen is a key factor required for alkene hydrogenation.

In Figs. 8a and b, we plot the molecular desorption signals of C_5H_{10} and D_2, observed for individual adsorption on Pd(111) and Pd particles, and of pentane-d_2 observed in the coadsorption experiments on the particles. It is clear that pentane is formed and desorbs from the Pd particles over a temperature range where the C_5H_{10} and D_2 desorption states overlap. This overlap is practically not fulfilled for the Pd(111) crystal due to the absence of weakly bonded hydrogen, and as a result the hydrogenation reaction does not occur. Therefore, the pentene hydrogenation reaction requires that weakly bound hydrogen is present on the surface before the pentene molecules desorb intact on heating.

This model of overlapping desorption states has been previously suggested to explain the results for ethene hydrogenation on the similarly prepared Pd particles [28]. We have observed that hydrogenation occurs when the overlap is present between hydrogen and weakly bound ethene as shown in Fig. 8d. The fact that trace amounts of ethane were observed on D/Pd(111) at 270 K (see Fig. 8c) and on H/Pd(110) at 250 K [32] indicates that there is a reaction pathway for the ethene hydrogenation via ethyl groups as well. However, in the presence of the subsurface H reservoir the reaction predominately occurs between π-pentene and weakly bound hydrogen resulting in much more ethane production desorbing at 200 K.

The results presented in this paper show that pentene hydrogenation proceeds via half-hydrogenated alkyl species formed from strongly bound di-σ-pentene. Meanwhile, it is generally believed that π-bonded ethene hydrogenates to ethane [3,20,44,45]. In other words, there must be overlap between the *active* species involved in the reaction. Therefore, the model of alkene and hydrogen overlapping desorption states may predict both the feasibility of alkene hydrogenation and the active species involved.

4. Summary

We have studied the adsorption properties of ethene, *trans*-2-pentene, *cis*-2-pentene, and 1-pentene on Pd(111) crystals and Pd particles supported on a thin alumina film by TPD. Each pentene isomer reacts in an identical manner. Three adsorption states are observed and are assigned to multilayer (desorbing at $\sim$ 130 K), π-bonded pentene ($\sim$ 180 K) and interchanging di-σ-bonded pentene/pentyl groups ($\sim$ 250 K). The latter species undergo coverage dependent stepwise dehydrogenation, which extends to $\sim$ 900 K for complete decomposition at saturated exposures.

Preadsorbed D_2 reduces the quantity of pentene that dehydrogenates and enhances molecular desorption of π-bonded pentene. For pentenes on D_2 preadsorbed Pd(111), the H–D exchange reaction occurs below 250 K, result-

ing in D-substituted pentene, which molecularly desorbs or dehydrogenates on heating similar to nonexchanged pentene. D_2 preadsorption suppresses the formation of the pentyl/pentene state. Pentane is not formed as a hydrogenation product on Pd(111).

On Pd nanoparticles, the dehydrogenation temperatures are found to be much lower ($\sim$ 130 K) than on Pd(111), implying that dehydrogenation proceeds more readily. In addition, the extent of the H–D exchange reaction is considerably greater on particles. In contrast to the Pd(111) crystal, the hydrogenation reaction occurs on the Pd particles. Data show that the di-σ-bonded pentene group is the precursor for H–D exchange and pentane formation, with both occurring via a pentyl group. This pentyl group reacts either by β-H elimination to form pentene or by reductive elimination to form pentane.

The results for pentene are compared with those obtained for ethene. Again, the hydrogenation of ethene is not observed on Pd(111), but it does occur on Pd particles. We have shown that the formation of weakly bonded subsurface hydrogen is the key factor required for the hydrogenation reaction to occur. The accessibility of these hydrogen atoms is enhanced on the particles due to the nanoscale dimensions. It should be noted however, that under atmospheric reaction conditions, the hydrogenation may also occur on Pd crystals, due to the enhanced accessibility of subsurface hydrogen at elevated pressures.

The results are rationalized on the basis of a model of overlapping desorption states, which may predict the feasibility of alkene hydrogenation on Pd catalysts and the active species involved in this reaction.

Acknowledgments

We acknowledge support by the ATHENA project funded by the Engineering & Physical Sciences Research Council (EPSRC) of the UK and Johnson Matthey plc. We also thank Prof. S.D. Jackson for fruitful discussions.

References

[1] V. Ponec, G.C. Bond, Catalysis by Metals and Alloys, Elsevier, Amsterdam, 1995.
[2] J. Horiuti, M. Polanyi, Trans. Faraday Soc. 30 (1934) 1164.
[3] G.A. Somorjai, Introduction to Surface Chemistry and Catalysis, Wiley, New York, 1994.
[4] D.R. Rainer, D.W. Goodman, J. Mol. Catal. A 131 (1998) 259.
[5] M. Frank, M. Bäumer, Phys. Chem. Chem. Phys. 2 (2000) 3723.
[6] F. Zaera, Progr. Surf. Sci. 69 (2001) 1.
[7] N. Sheppard, C. De La Cruz, Adv. Catal. 41 (1996) 1.
[8] N. Sheppard, C. De La Cruz, Adv. Catal. 42 (1998) 181.
[9] M. Neurock, R.A. van Santen, J. Phys. Chem. B 104 (2000) 11127.
[10] W.T. Tysoe, G.L. Nyberg, R.M. Lambert, J. Phys. Chem. 88 (1984) 1960.
[11] D. Stacchiola, L. Burkholder, W.T. Tysoe, Surf. Sci. 511 (2002) 215.
[12] D. Stacchiola, W.T. Tysoe, Surf. Sci. 540 (2003) L600.
[13] M. Sock, A. Eichler, S. Surnev, J.N. Andersen, B. Klötzer, K. Hayek, M.G. Ramsey, F.P. Netzer, Surf. Sci. 545 (2003) 122.
[14] J.A. Gates, L.L. Kesmodel, Surf. Sci. 120 (1982) L461.
[15] J.A. Gates, L.L. Kesmodel, Surf. Sci. 124 (1983) 68.
[16] B. Tardy, J.C. Bertolini, J. Chem. Phys. 82 (1985) 407.
[17] M.A. Chesters, G.S. McDougall, M.E. Pemble, N. Sheppard, Appl. Surf. Sci. 22/23 (1985) 369.
[18] M. Nishijima, J. Yoshinobu, Sekitani, M. Onchi, J. Chem. Phys. 90 (1989) 5114.
[19] E.M. Stuve, R.J. Madix, C.R. Brundle, Surf. Sci. 152/153 (1985) 532.
[20] T.P. Beebe, J.T. Yates Jr., J. Am. Chem. Soc. 108 (1986) 663.
[21] N.A. Thornburg, I.M. Abdelrehim, D.P. Land, J. Phys. Chem. B 103 (1999) 8894.
[22] D. Stacchiola, L. Burkholder, W.T. Tysoe, Surf. Sci. 542 (2003) 129.
[23] X.-C. Guo, R.J. Madix, J. Catal. 155 (1995) 336.
[24] N. Vasquez Jr., R.J. Madix, J. Catal. 178 (1998) 234.
[25] M. Bäumer, H.-J. Freund, Progr. Surf. Sci. 61 (1999) 127.
[26] C.T. Campbell, Surf. Sci. Rep. 27 (1997) 1.
[27] S.K. Shaikhutdinov, M. Heemeier, M. Bäumer, T. Lear, D. Lennon, R.J. Oldman, S.D. Jackson, H.-J. Freund, J. Catal. 200 (2001) 350.
[28] S.K. Shaikhutdinov, M. Frank, M. Bäumer, S.D. Jackson, R.J. Oldman, J.C. Hemminger, H.-J. Freund, Catal. Lett. 80 (2002) 115.
[29] A.M. Doyle, S.K. Shaikhutdinov, S.D. Jackson, H.-J. Freund, Angew. Chem. Int. Ed. 42 (2003) 5240.
[30] See web-site http://webbook.nist.gov.
[31] M.X. Yang, M. Xi, H. Yuan, B.E. Bent, P. Stevens, J.M. White, Surf. Sci. 341 (1995) 9.
[32] D. Chrysostomou, F. Zaera, Surf. Sci. 457 (2000) 89.
[33] T. Sekitani, T. Takaoka, M. Fujisawa, M. Nishijima, J. Phys. Chem. 96 (1992) 8462.
[34] M. Heemeier, S. Stempel, S.K. Shaikhutdinov, J. Libuda, M. Bäumer, R.J. Oldman, S.D. Jackson, H.-J. Freund, Surf. Sci. 523 (2003) 103.
[35] K. Christmann, in: Z. Paal, P.G. Menon (Eds.), Hydrogen Effects in Catalysis, Dekker, New York, 1988, p. 3.
[36] G.E. Gdowski, T.E. Felter, R.H. Stulen, Surf. Sci. 181 (1987) L147.
[37] H. Okuyama, W. Siga, N. Takagi, M. Nishijima, T. Aruga, Surf. Sci. 401 (1998) 344.
[38] U. Muschiol, P.K. Schmidt, K. Christmann, Surf. Sci. 395 (1998) 182.
[39] R.J. Behm, V. Penka, M.-G. Cattania, K. Christmann, G. Ertl, J. Chem. Phys. 78 (1983) 12.
[40] D. Farias, M. Patting, K.H. Rieder, Phys. Status Solidi 159 (1997) 255.
[41] M. Wilde, M. Matsumoto, K. Fukutani, T. Aruga, Surf. Sci. 482/485 (2001) 346.
[42] M.S. Daw, S.M. Foiles, Phys. Rev. B 35 (1987) 2128.
[43] K. Wolter, PhD thesis, Frei Universität, Berlin, 2001.
[44] P.S. Cremer, G.A. Somorjai, J. Chem. Soc., Faraday Trans. 91 (1995) 3671.
[45] H.-J. Freund, M. Bäumer, J. Libuda, T. Risse, G. Rupprechter, S. Shaikhutdinov, J. Catal. 216 (2003) 223.